FINAL REPORT

Clarence Karr, Jr.
Principal Investigator
U.S. Bureau of Mines
Morgantown, West Virginia 26505

CONTRACT No. T-88614

FINAL REPORT
CONTRACT NO. T-88614

INFRARED VIBRATIONAL SPECTROSCOPIC STUDIES OF MINERALS FROM APOLLO 11 AND 12 LUNAR SAMPLES

Patricia A. Estep, John J. Kovach and Clarence Karr, Jr.

Morgantown Energy Research Center

U. S. Department of the Interior

Bureau of Mines

Morgantown, West Virginia 26505, U. S. A.

4 Tables, 7 Figures

Reviews and Proofs to: Patricia A. Estep

Morgantown Energy Research Center

U. S. Department of the Interior

Bureau of Mines

P. O. Box 880

Collins Ferry Road

Morgantown, West Virginia 26505

Telephone:

(Office) - 304/599-3441, Extension 348

(Home) - 304/599-0663

OUTLINE

Abstract (small print)

INTRODUCTION

EXPERIMENTAL (small print)

Mineral Separations

Polish Preparation

RESULTS AND DISCUSSION

Structure Determination of Mineral Separates

(a) Pyroxenes

(b) Plagioclase Feldspars

(c) Olivines

(d) Ilmenite

Determination of Bulk Composition of Composite Samples

(a) Dust Grains and Sieved Fractions

(b) Glasses

Attached: 7 figures

4 tables

Captions for figures (small print)

23 references

acknowledgments

Abstract

Infrared vibrational spectral correlations, derived from terrestrial and synthetic minerals, were used to characterize structures of the predominant lunar silicate minerals isolated from crystalline rocks and dusts. Absorption bands in the low-frequency region (400-180 cm^{-1}) were used to determine specific compositions for isolated pyroxene (Fs_{21} to Fs_{37}), plagioclase (An_{81} to An_{100}), and olivine (Fa_{28} to Fa_{34}). For each of these predominant minerals, spectral similarities for separates from both rocks and dusts were observed. Further correlations from the fundamental vibrations of silicate SiO_4 tetrahedra were used to determine basic compositions for bulk samples from the dusts. The distinctive lunar basaltic spectra, predominant in pyroxene, matched better with some ocean tholeiitic basalts than with tektites, meteorites, or any other terrestrial rock type, but in no case was a good composition obtained.

Iron composition variations in lunar pyroxenes produced spectral changes that were color related and may be correlatable with distribution of cations over the nonequivalent octahedrally coordinated sites. Colors of lunar glass were also observed to be composition dependent, and infrared spectral evidence is given to support the origin of light glass from plagioclase and dark glass from pyroxenes. Spectra of lunar glass were markedly different from those of tektites.

INTRODUCTION

This paper reports the first application of infrared vibrational spectroscopy to the analysis of lunar samples. The potential of this method for the structural analysis of rocks and minerals that could be found on the lunar surface was previously demonstrated by LYON (1963) for the mid-infrared region to 400 cm^{-1}. The recently developed easy accessibility of the low-frequency far-infrared region to 30 cm^{-1} has further contributed to the usefulness of infrared spectroscopy in determining specific molecular structure of minerals. We have characterized the structures of the predominant lunar silicate minerals of pyroxene, plagioclase, and olivine, isolated from both rocks and dusts, through use of infrared spectral-structural correlations derived from terrestrial and synthetic minerals. Cation substitutions in these silicates were determined from data obtained in the low-frequency vibration region. We used spectra of the separated minerals and further correlations from the fundamental vibrations of silicate SiO_4 tetrahedra to classify bulk compositions of dust sieved fractions, composite grains and glass particles. Cation ordering in some lunar pyroxene and plagioclase separates was indicated from changes in infrared absorption band shapes, resolution and intensities. Such information on atomic

distributions over the structural sites is useful in deducing formation conditions for these lunar minerals and can contribute to reconstructing the moon's early history.

EXPERIMENTAL

Mineral Separations

All lunar samples were handled, and pellets were prepared in a glove box purged with dry nitrogen. Available for our infrared studies were one Apollo 11 dust (10085-46) and six Apollo 12 samples: Three crystalline rocks (12018-26, 12020-26, 12021-24) and three lunar dusts (12001-60, 12057-57, 12070-24). The dusts were dry-sieved to obtain mineral separates of a size suitable for microscopic isolation (10-60X) and infrared analysis. Grain size distribution data for the four dusts are given in Table 1. For the three Apollo 12 dusts, a statistical two-way contingency test of the data (conducted at the 95% confidence level) showed that dusts 12070-24 (contingency sample) and 12057-57 (documented sample) (both appearing to be bimodal) have the same distribution, but their distributions are different from that of dust 12001-60 (selected sample). Dust mineral grains were microscopically separated only from the +100 mesh sieved fractions, and ranged 1600 to 150μm for the Apollo 12 dusts. A single grain of about 1300 μm was necessary to give the 1 milligram of sample required for a good mid-infrared spectrum. A typical dust grain size of 250 μm required 50 combined grains. Data from a number of selections, relating number and size of grains required for 1 milligram, were plotted and used as working

curves to facilitate subsequent microscopic isolations. Crystalline fragments chipped from rock samples gave single phases typically 300 μm and ranging 900 to 50 μm. About 40 of these were required for a mid-infrared spectrum.

Pellet Preparation

Isolated mineral grains were placed in a mullite mortar fitted with a specially designed stainless steel funneled cylinder. A 3mm diameter plunger was tapped lightly down through the cylinder onto the confined sample, producing completely recoverable crushed fragments directly on the mortar surface. The cylinder assembly was removed and further hand grinding continued in the same mortar in order to reduce particle size to an estimated 10-20μm. To prepare a pellet for the mid-infrared region (4000-200 cm^{-1}), 500 milligrams of powdered cesium iodide (Harshaw Chemical Co.) were added directly to the preground sample in the mortar and the mixture blended for 5 minutes. This mixture was triple pressed in a die at 23,000 lbs total, with a 15-minute total press time. The resulting 13mm diameter x 0.8mm thick pellet was placed in a cell specially constructed to exclude air, and scanned on a Perkin-Elmer 621 grating spectrophotometer*, purged with dry air. A comparison of

*Reference to specific equipment is made to facilitate understanding and does not imply endorsement by the Bureau of Mines.

spectra obtained for pellets mounted in this special holder with those of pellets exposed to the atmosphere in a regular pellet holder showed no detectable structural changes. Therefore, all subsequent cesium iodide pellets were scanned exposed to dry air. Pellets for far-infrared spectra were prepared in a similar manner, using 4 milligrams of sample and 150 milligrams of polyethylene (Uvasol, E. Merck AG) as a pellet matrix. The 1-inch-diameter pellets were scanned on a Perkin-Elmer FIS-3 vacuum spectrophotometer, covering the range 400 to 30 cm^{-1}.

RESULTS AND DISCUSSION

Structure Determination of Mineral Separates

Pyroxene, plagioclase, olivine and ilmenite (in order of decreasing abundance) were isolated from the lunar rocks and dusts and these were readily identified from their distinctive infrared spectra. Table 2 lists absorption band frequencies for some separates of each of these minerals and Figure 1 gives examples of spectra for the predominant lunar silicates. Absorption bands appearing in the infrared spectrum of a silicate structure are commonly assigned to vibrations of SiO_4 tetrahedra, to octahedra or tetrahedra of substituted cations (metal-oxygen bonds) and to lattice vibrations. The frequencies of all these absorption bands can be affected by changes in cation substitution through changes in bond distances and bond force constants. This sensitivity to small changes in molecular structure allowed us to determine some specific cation substitutions for each of the predominant lunar silicate minerals. Correlation curves based on composition dependent frequency shifts were derived from a number of synthetic and terrestrial standards for each of the silicate classes. These were then applied in a determination of specific chemical composition for individual lunar separates after the silicate molecular structure was established from overall spectral features. The absorption bands selected for use

in the cation determinative curves were all from the low-frequency region 400-180 cm^{-1} and are shown starred in Figure 1. Although these varied medium to weak in absorption intensities, they were selected as the most suitable compromise between maximum frequency shifts with compositional changes and best fits of the data to the determinative curves.

(a) Pyroxenes

Pyroxenes were isolated as colored transparent angular fragments from the rocks and dusts listed in Table 3. All spectra were similar to that shown in Figure 1 curve (b) in band shapes and relative intensities. These pyroxene spectra more closely matched those of a series of seven synthetic pigeonites that we studied in the composition range $Wo_{10}En_{75}Fs_{15}$ to $Wo_{10}En_{30}Fs_{60}$ (Tem-Pres Research Division, The Carborundum Co., State College, Pennsylvania) than those of any other pyroxenes with which we compared them. Spectra of terrestrial calcic clinopyroxenes, e.g., a series falling in composition along the diopside-hedenbergite tie line (sample from G.M. Bancroft) did not compare with spectra of the lunar pyroxenes that we isolated. Similarly, spectra of a series of terrestrial aluminous augites and salites from metamorphic rocks with extensive and varied cation substitutions

(Wo_{43} to Wo_{56}, with 2.2 to 13.5 % Al_2O_3, A. T. Rao, Andhra University, Waltair, India) (RAO, 1969), all differed markedly from those of lunar pyroxenes. A volcanic augite from Kakanui, New Zealand ($Wo_{30}En_{45}Fs_{10}$), also with substantial cation substitution and showing a more band-broadened spectrum than the metamorphic clinopyroxenes because of its disorder (HAFNER AND VIRGO, 1970), did not match well with lunar pyroxenes. Spectra of the calcium-poor clinopyroxenes, clinoenstatite (synthetic and natural) and clinohypersthene (synthetic), as well as spectra of orthopyroxenes from enstatite to hypersthene ($Fs_{14.5}$ to $Fs_{85.9}$, same sample studied by BANCROFT et al, 1967; LYON, 1963) did not compare well with that of lunar pyroxenes.

The chemical inhomogeneity of pyroxenes due to compositional zoning has been described by BENCE et al., (1970) for rock 12021 and by other workers for lunar pyroxenes. Since it was necessary to combine several grains for a single infrared analysis, the spectra therefore represent the predominant composition for the pyroxene separates and thus yield modal information. Although other workers have reported the identification of pyroxene in the augite range, we tentatively conclude that the predominant compositions of our pyroxene separates lie in the pigeonite to subcalcic augite range, based on the above described spectral comparisons. Studies on

synthetic augites and sub-calcic augites are in progress to determine the effects on infrared spectra of systematic changes in calcium content and aluminum substitution into these structures. An example of the closely matching general features of lunar pyroxene spectra with those of the synthetic pigeonites is shown in Figure 2. Curve (c) is the spectrum of dark amber pyroxene fragments isolated from rock 12018-26 and these appear to be intermediate in band shapes, resolution and frequencies, between the synthetic pigeonites with iron contents of Fs_{30} and Fs_{38}. We observed that as the color of lunar pyroxenes progressively deepened from yellow to dark amber, nearly all absorption bands systematically shifted to lower frequencies (Table 2). Studies on the closely matching synthetic pigeonites showed that these frequency decreases are related to increasing Fe^{2+} content. The decrease in bond energies in this silicate structure results from the replacement of smaller (0.72Å) and lighter Mg^{2+} ions by larger (0.77Å) and heavier Fe^{2+} ions. We selected the absorption band shifting from 400 to 368 cm^{-1} in synthetic pigeonites Fs_{15} to Fs_{60} (Fig. 2), for use in a cation determinative curve, shown in Figure 3. The observed range of 394 to 380 cm^{-1} for this absorption band in lunar pyroxene separates indicated Fe^{2+} compositions in the range Fs_{21} to Fs_{37}. Specific frequency ranges

observed for various colors of lunar pyroxenes are shown in Figure 3 to demonstrate the correlation of color with Fe^{2+} content. We studied this same analytical absorption band in orthopyroxene spectra and observed the same correlation between Fe^{2+} content and frequencies. The decrease in Ca^{2+} content and the change to orthorhombic crystal system shifted frequencies for the analytical absorption band very little from those of the monoclinic pyroxenes.

In addition to frequency shifts with increasing Fe^{2+} content, we observed in spectra of both lunar clinopyroxenes and the series of synthetic clinopyroxenes (Fig. 2), that there is progressive band broadening and a systematic decrease of absorption intensities with increasing Fe^{2+} content (yellow to amber for lunar pyroxenes). These effects could be due to the increasing nonequivalence of neighboring chains in the pyroxene structure, known to occur with increasing Fe^{2+} substitution (MORIMOTO, 1960). Mossbauer data for terrestrial orthopyroxenes (BANCROFT ET AL, 1967) and lunar clinopyroxenes (HAFNER AND VIRGO, 1970) show that increasing Fe^{2+} content is accompanied by a more disordered Fe^{2+} distribution over the nonequivalent octahedrally coordinated sites, M1 and M2. If the observed broadening and intensity decrease of infrared absorption bands in clinopyroxenes is related to this same phenomenon, then the well-resolved spectrum obtained for the iron-poor yellow lunar pyroxenes (e.g., curve (b) (Fig. 1) suggests a relatively ordered structure.

From their Mössbauer studies, HAFNER and VIRGO (1970) have interpreted cation ordering in lunar pyroxenes as an indication of slow cooling at relatively low equilibrium temperatures. The synthetic clinopyroxenes, soaked up to 288 hours at 850° C and slow-cooled, are expected to have achieved equilibrated distributions of cations over the nonequivalent sites. Further support from infrared data for ordering in lunar pyroxenes was obtained by comparison with a terrestrial volcanic pigeonite

$$Ca_{0.29}Na_{0.02}K_{0.01}Mn_{0.02}Mg_{0.92}Fe^{2+}_{0.74}Al_{0.06}Si_{1.94}O_6$$

(Hakone Volcano, Japan, No. 101824) determined to be appreciably ordered from Mössbauer studies (BANCROFT and BURNS, 1967). The spectrum of this pigeonite compares with lunar pyroxene spectra in frequencies, overall band shapes and resolution nearly as well as the synthetic pigeonites. All other terrestrial pigeonite samples that we studied, presumably with more rapid cooling histories, exhibited band-broadened spectra, suggesting considerable disorder.

Thus the infrared comparisons that we made indicate that the lunar pyroxenes isolated were monoclinic, calcium-poor, ranging in iron composition Fs_{21} to Fs_{37}, probably more ordered for the iron-poor pyroxenes, and similar in scructure from samples of both rocks and dusts.

(b) Plagioclase Feldspars

Plagioclase feldspars were isolated from the rocks and dusts listed in Table 3, varying typically from colorless transparent fragments to white-grey opaque grains. The spectrum of a single chalky-white, black-flecked anorthite grain (An_{100}) isolated from the Apollo 11 lunar dust is shown in Figure 1, curve (a). Its unusually well-resolved spectral features in both the mid- and far-infrared regions (to 30 cm^{-1}) indicated that this particular lunar plagioclase sample was more highly ordered (in Si/Al distribution) than most of the lunar plagioclase, or that in any of the terrestrial anorthosites or anorthite specimens that we studied. Previous systematic studies of the variation of infrared spectra of plagioclase feldspar with composition (THOMPSON, 1967; ANGINO, 1969) and data from this laboratory on analyzed terrestrial plagioclase samples indicated that the absorption band shown starred in curve (a), Figure 1, was a good choice for a determinative curve. This band shifts linearly from 185 to 235 cm^{-1} (An_5 to An_{95}) with increasing Ca^{2+} content of the plagioclase ($\nu_{cm^{-1}} = 180.35 + 0.5637\ An_{\text{mole percent}}$). The shift does not reflect simple mass or ionic radii effects and may be related to increasing substitution of Al^{3+} in the more calcic plagioclase (ANGINO, 1969). Observed frequencies of 226 to 237 cm^{-1} for the lunar plagioclase separates were applied to the determinative curve and these indicated bytownite to pure anorthite, An_{81} to An_{100}.

We compared spectra of several anorthositic and gabbroic anorthositic grains isolated from dust 12070-24 with those from three types of terrestrial anorthosites; massive Adirondak (An_{44} to An_{56}, Y. W. Isachsen, University of the State of New York); stratiform Bushveld (An_{95}, J. Ferguson, University of Witwatersrand, South Africa); and Group III anorthosites from West Greenland (An_{47} to An_{96}, B. F. Windley, University of Leicester, England). The latter have been suggested to be the first terrestrial rocks to have any marked affinities with those on the moon (WINDLEY, 1970). The Bushveld (An_{95}) and some Greenland (An_{92} to An_{96}) anorthosite spectra compared favorably with lunar anorthosite spectra because of their high anorthite contents. We also obtained a good match of lunar anorthositic spectra with those of two eucrites, Sioux Co., Nebraska and Pasamonte, New Mexico, that were both predominant in calcic plagioclase (An_{95}).

(c) Olivines

Olivines were isolated from the lunar rocks and dusts listed in Table 3, with varied morphologies. Their infrared spectra, e.g., curve (c), Figure 1, showed them to be in the forsterite-fayalite olivine series. Spectra were similar for separates from both rocks and dusts. As with pyroxenes, frequencies of olivine bands are composition dependent (DUKE and STEVENS, 1964; BURNS and HUGGINS, 1970) and decrease as Fe^{2+} content increases. We

selected for use in a cation determinative curve the low-frequency absorption band shown starred in curve (c), Figure 1. The correlation curve ($\nu_{cm^{-1}} = 419 - 0.653\ Fa_{\text{mole percent}}$) was determined from a series of nine synthetic olivines in the Fe-Mg series (Tem-Pres Research), in which this absorption band shifted linearly from 418 to 356 cm^{-1} for Fa_0 to Fa_{100}. For lunar olivine separates this band ranged 401 to 397 cm^{-1}, indicating a narrow composition range of Fa_{28} to Fa_{34} from the correlation plot. We compared lunar olivine compositions with those of a series of 32 chondrites that we examined, which varied from Fa_{14} to Fa_{29} (410 to 400 cm^{-1}) in agreement with values reported for most chondrites by MASON (1962). Only six other chondrites that we studied, with frequencies in the range 395 to 387 cm^{-1}, had higher fayalite compositions of Fa_{37} to Fa_{49}. Thus the fayalite content of the lunar olivines that we isolated comprise a narrower composition range than for the meteorites that we studied and fell within the apparent gap of Fa_{29} to Fa_{37} that we found for these meteorites.

(d) Ilmenite

Ilmenite occurred as fine grains in rocks and dusts (Table 3) and was typically isolated in fragments averaging 100μm, still associated with trace amounts of unidentified silicates (1093, 1065 and 1050 cm^{-1}). A typical isolation required 324 grains to obtain enough for a mid-infrared spectrum. We have observed significant variations in terrestrial ilmenite spectra for both natural and synthetically prepared samples, with frequency shifts up to 30 cm^{-1}. These infrared differences may be related to subtle structure variations and further characterization of the lunar ilmenite structure beyond a straightforward identification may be possible from a thorough study of these effects.

Determination of Bulk Composition of Composite Lunar Samples

We obtained infrared spectra of the lunar dust composite samples listed in Table 4 for comparison with a variety of samples. To facilitate these comparisons we used the stretching vibrations of Si-O bonds in silicate SiO_4 tetrahedra, appearing in the frequency range of 1200 to 800 cm^{-1}, for classification of bulk compositions. These intense vibrations are highly sensitive to changes in bond force constants and (LYON, 1965) has shown that their frequency shifts can be correlated with SiO_2 content. Figure 4 shows this general correlation applied to a wide range of bulk compositions and the plot includes 133 samples of terrestrial rocks, synthetic glasses, tektites and meteorites. The correlation was found to apply to samples that

are highly crystalline, glassy, fine-grained or coarse-grained. Samples with high SiO_2 content, such as acid rocks, tektites and synthetic glasses (blocks D, E, F) are found at higher frequencies, while low SiO_2 content samples such as meteorites, basalts, gabbros and other basic rocks (blocks A, B, C) appear at considerably lower frequencies. This shift of the Si-O stretching vibration reflects both chemical and mineralogical compositions, showing a decrease in frequency as the Si/O mole ratio decreases (0.5 to 0.25) in going from tektosilicates to nesosilicates (LAUNER, 1952; SAKSENA, 1959). The frequency decrease reflects a decrease in the "degree of polymerization" of SiO_4 tetrahedra in a silicate lattice and consequently, decreasing bond energies. For example in Figure 1, the center of gravity for the Si-O stretching vibration is seen to decrease 1010 cm^{-1}, 980 cm^{-1} to 930 cm^{-1} for plagioclase (tektosilicate), pyroxene (inosilicate) to olivine (nesosilicate), respectively. Substitution of cations into a silicate structure, whether replacement for Si in the tetrahedra or substitution into octahedral sites, results in lower Si-O stretching frequencies (MILKEY, 1960; STUBICAN, 1961). Heavy cations such as Fe^{2+} and Ti found in basalts and gabbros decrease the Si-O stretching frequency more than lighter cations.

(a) Dust Grains and Sieved Fractions

We used this frequency-silica content correlation and comparisons of other overall spectral features to classify compositions of composite samples from the lunar dusts. Si-O stretching frequencies for individual dust grains and sieved dust fractions ranged 1005 to 975 cm^{-1} (Table 4) and these indicated basic to ultrabasic compositions of 52 to 40 % SiO_2, from the correlation plot in Figure 4. Although gross spectral features classify the lunar samples as basaltic, in no case was an exact comparison obtained with spectra of any of the large number of terrestrial rock types with which we compared them. The distinctive lunar basaltic spectrum, as shown for example in Figure 5 curve (a), compared more favorably in general features with that of some ocean tholeiitic basalts (curve b) than with most samples. It was markedly different from that of olivine-rich chondrites (curve c), tektites (curve d) and plagioclase-rich eucrites.

Isolated basaltic grains ranged from microgranular grey aggregates to dark grey-brown blocky fragments and their spectra were similar to each other, and also to the dust sieved fractions as shown for example in Figure 6, curves (b) and (c), for dust 12070-24. These unique basalt type spectra appear to be dominated by pyroxenes as shown in Figure 6 by comparison with the spectrum of a pyroxene (Fs_{27}) (curve a) isolated from the same dust. The slight shifts of

the medium intensity absorption band in the Si-O-Si bending region to lower frequencies (500 to 467 cm^{-1}) in some sieved dust fractions (see Table 4) may be associated with increasing iron content, as observed for the lunar pyroxene separates.

(b) Glasses

Glasses were isolated from the lunar dusts listed in Table 4 as beads (700 to 200 μm) and irregular fragments. Si-O stretching frequencies in the range 1000 to 960 cm^{-1} similarly classified these as basaltic compositions from the correlation plot in Figure 4 (50 to 34% SiO_2). For Apollo 11 glasses, a trend of increasing depth of color with increasing iron substitution and decreasing SiO_2 content has been reported (ANDERSON et al, 1970; VON ENGLEHARDT et al, 1970) and the data in Table 4 show this correlation. For the glasses isolated from the Apollo 11 sample, the decrease of the Si-O stretching frequency from 1000 cm^{-1} for light-colored glass to 960 cm^{-1} for dark-colored glass indicates decreasing SiO_2 content from Figure 4 (50 to 34%), and is presumably associated with increasing iron substitution. This color correlation also applied in the case of the two Apollo 12 glasses even though fine structure appearing on the major silicate absorption bands suggested some devitrification. The Si-O stretching frequency for light-colored glass (1000 to 990 cm^{-1}) approximates that of lunar plagioclase (1010 cm^{-1}), while that of the dark-colored glass (972 to 960 cm^{-1}) approximates

that of lunar pyroxenes (980 to 970 cm^{-1}), supporting the belief that these two types of glass are formed from these minerals. We compared spectra of the lunar glasses with that of 24 tektites and a suite of eight pseudo-lunar artificial glasses synthesized by Greene (Fig. 4) to approximate the surface composition of Mare Tranquillitatis (TURKEVICH, 1969). The examples in Figure 7 demonstrate the better match in frequencies and band shapes of lunar glass spectra with those of the pseudo-lunar glasses than with those of tektites. The higher frequencies for the Si-O stretching vibrations in tektites (1070 to 1055 cm^{-1}) reflect their higher SiO_2 content (70 to 80%), as compared with that of the pseudo-lunar glasses that we studied (54 to 46% SiO_2, 1000 to 980 cm^{-1}) (See Figure 4). Frequencies for the three predominant absorption bands in the 24 tektites that we studied did not vary more than 15 cm^{-1}.

Acknowledgments

We thank Edward E. Childers and Arthur L. Hiser of this laboratory for isolating and obtaining spectra on terrestrial minerals and rocks, and John J. Renton, West Virginia University, for authenticating structures of terrestrial minerals by X-ray diffraction. We are grateful to R. G. Burns, Massachusetts Institute of Technology, G. M. Bancroft, University of Western Ontario, Canada, J. S. White, Smithsonian Institution, and J. D. Stevens, Kennecott Copper Corporation, for supplying pyroxene samples; to F. C. Dehn, PPG Industries, for terrestrial ilmenite samples; to W. R. Riedel, Scripps Institution of Oceanography, for ocean basalts; to C. H. R. von Koenigswald, Forschungs-Institut Senckenberg, Germany, D. R. Chapman, NASA, Ames Research Center, and C. B. Moore, Arizona State University, for tektite samples; to E. J. Olsen, Chicago Natural History Museum, for rare meteorite samples; and to many others (as noted in the text) who generously supplied analyzed samples for our comparisons. This research was sponsored by NASA under Contract No. T-88614.

REFERENCES

ANDERSON, O. L., SCHOLZ, C., SOGA, N., WARREN, N., and SCHREIBER, E. (1970) Elastic properties of a micro-breccia, igneous rock and lunar fines from Apollo 11 mission. Proc. Apollo 11 Lunar Sci. Conf., Geochim. Cosmochim. Acta. Suppl. 1, 3, 1959-1973. Pergamon.

ANGINIO, E. E. (1969) Far infrared absorption spectra of plagioclase feldspars. Kansas Geol. Surv. Bull. Pt. 1, 194, 9-11.

BANCROFT, G. M. and BURNS, R. G. (1967) Distribution of iron cations in a volcanic pigeonite by Mössbauer spectroscopy. Earth and Planetary Sci. Letters 3, 125-127.

BANCROFT, G. M., BURNS, R. C., and HOWIE, R. A. (1967) Determination of the cation distribution in the orthopyroxene series by the Mössbauer effect. Nature 213, 1221-1223.

BENCE, A. E., PAPIKE, J. J., and PREWITT, C. T. (1970) Apollo 12 clinopyroxenes: chemical trends. Earth and Planetary Sci. Letters 8, 393-399.

BURNS, R. G., and HUGGINS, F. E. (1970) Cation determinative curves and evidence of ordering in Mg-Fe-Mn olivines from vibrational spectra. Pres. Nov. 3, 1970, Geol. Soc. of Am. Symp. on Crystal Chem. of Silicates, Milwaukee, Wisconsin, Am. Mineralogist, In Press.

REFERENCES (Continued)

DUKE, D. A. and STEPHENS, J. D. (1964) Infrared investigation of the olivine group minerals. Amer. Mineral. 49, 1388-1406.

HAFNER, S. S. and VIRGO, D. (1970) Temperature-dependent cation distribution in lunar and terrestrial pyroxenes. Proc. Apollo 11 Lunar Sci. Conf., Geochim. Cosmochim Acta. Suppl. 1, 3, 2183-2198. Pergamon.

LAUNER, P. J. (1952) Regularities in the infrared absorption spectra of silicate minerals. Amer. Mineral 37, 764-784.

LYON, R.J.P. (1963) Evaluation of infrared spectrophotometry for compositional analysis of lunar and planetary soils. Standford Res. Inst., Final Rept. under contract NASr-49 (04), Pub. by NASA as Tech. Note D-1871.

LYON, R.J.P. (1965) Analysis of rocks by spectral infrared emission (8 to 25 microns). Eco. Geol. 60, 715-736.

MASON, B. (1962) Meteorites. John Wiley & Sons, N. Y., 201, 62.

MILKEY, R.G. (1960) Infrared spectra of some tectosilicates. Amer. Mineral. 45, 990-1007.

MORIMOTO, NOBUO, APPLEMAN, D. E. and EVANS, H. T., JR. (1960) The crystal structures of clinoenstatite and pigeonite. Z.Kristallogr. 114, 120-147.

REFERENCES (Continued)

RAO, K.S.R., RAO, A.T., and SRIRAMADAS, A. (1969) Porphyritic plagioclase-hornblende-pyroxene graulite from charnockitic rocks of Chipurupalli, Visakhapatnam District, Andhra Pradesh, South India. Mineral. Mag. 37, 497-503.

SAKSENA, B.D. (1959) Classification of silicate structures from infrared studies. Proc. of Symp. on Raman & Infrared Spectroscopy, Nainital, 93-102.

STUBICAN, B. and ROY, R. (1961) Infrared spectra of layer-structure silicates. J. Amer. Ceram. Soc. 44, 625-627.

THOMPSON, C.S. (1967) Determination of the composition of plagioclase feldspars by means of infrared spectroscopy. Ph.D. Disser., Univ. of Utah.

TURKEVICH, E.J., FRANZGROTE, J., and PATTERSON, J.H. (1969) Chemical composition of the lunar surface in mare tranquillitatis. Sci. 165, 277-279.

UREY, H.C., and CRAIG, H. (1953) The composition of the stone meteorites and the origin of the meteorites. Geochim. Cosmochim. Acta. 4, 36-82.

VIRGO, D., HAFNER, S.S., and WARBURTON, D. Cation distribution studies in clinopyroxenes, olivines and feldspars using Mössbauer spectroscopy of ^{57}Fe. Apollo 12 Lunar Sci. Conf. (unpublished proceedings).

REFERENCES (Continued)

VONENGLEHARDT, W., ARNDT, J., MULLER, W. F., and STOFFLER, D. (1970) Shock metamorphism in lunar samples. Sci. 167, 669-670.

WINDLEY, B. F. (1970) Anorthosites in the early crust of the earth and the moon. Nature 226, 333-335.

Table 1. Grain size distribution for lunar dusts

Screen size, mesh	Grain size, μm	Weight percent of total dust			
		12001-60	12057-57	12070-24	10085-46
+100	>149	29.92	27.55	21.73	91.5
+200 -100	149-74	23.80	28.09	24.10	n.d.*
+325 -200	74-44	18.87	18.05	19.46	n.d.
+400 -325	44-37	17.08	5.37	5.91	n.d.
-400	<37	10.32	20.93	28.80	n.d.

*n.d. = not determined: the +100 mesh fraction from dust 10085-46 (fines to coarse fines) contained larger grains (7000-150μm) than those for the three other dusts.

TABLE 2. Infrared Absorption Bands of Mineral Separates from Lunar Samples

Mineral Separate	Derived Composition	Source	Frequencies*, cm^{-1}
Pyroxene (yellow transparent angular fragments)	Fs_{22}	12021-24	240(w), 287(w), 310(w), 339(mw), 393(mw), 412(sh), 450(sh), 475(sh), 502(s), 545(sh), 638(mw), 669(w), 728(w), 882(s), 955(s), 1022(sh), 1055(s), 1130(sh)
Pyroxene (dark amber transparent angular fragments)	Fs_{37}	12021-24	235(w), 285(w), 321(mw), 380(w), 483(s), 535(sh), 628(mw), 658(w), 722(w), 875(s), 917(w), 960(s), 1053(s)
Plagioclase (single chalky-white grain)	An_{100}	10085-46	144(w), 166(vw), 179(vw), 192(vw), 209(w), 237(mw), 287(vw), 305(w), 318(w), 353(w), 380(w), 390(m), 400(w), 430(w), 455(w), 468(w), 483(w), 538(w), 577(m), 602(w), 622(m), 665(w), 680(w), 697(w), 728(w), 757(w), 926(s), 945(w), 965(w), 983(w), 1016(s), 1082(s), 1137(s)
Olivine (yellow transparent equant grains)	Fa_{33}	12018-26	283(w), 352(m), 398(m), 493(s), 510(s), 590(m), 832(w), 880(s), 938(w), 972(s), 1065(sh)

Table 2. Infrared absorption bands of mineral separates from lunar samples (con.)

Mineral separate	Derived composition	Source	Frequencies*, cm^{-1}
Ilmenite (black lustrous grains)		10085-46	285(m), 320(w), 365(w), 440(mw), 522(s), 675(mw)

*analytical frequencies used to derive chemical compositions are underlined.

s = strong

m = medium

w = weak

sh = shoulder

Table 3. Analyses of mineral separates from lunar rocks and dusts.

Mineral Isolated	Sample Source*	Description of mineral separates**	Number of analyses	Analytical frequencies cm^{-1}	Derived composition
Pyroxene	12018-26	Transparent light to dark amber angular fragments, 185μm; white granular opaque grain, composited with olivine, 350μm	3	392-385	$Fs_{23} - Fs_{30}$
	12021-24	Yellow to dark amber angular fragments, 650-250μm	9	393-380	$Fs_{22} - Fs_{37}$
	12070-24	Dark yellow to reddish amber angular fragments, 350-200μm	7	394-382	$Fs_{21} - Fs_{34}$
	10085-46	Medium to dark amber angular fragments, 300-150μm	4	388-385	$Fs_{27} - Fs_{30}$

Table 3. Analyses of mineral separates from lunar rocks and dusts (con.).

Mineral Isolated	Sample Source*	Description of mineral separates**	Number of analyses	Analytical frequencies cm^{-1}	Derived composition
Plagioclase	12018-26	Colorless transparent angular fragments, 160μm	1	228	An_{85}
	12021-24	Colorless transparent angular fragments, 450-320μm	5	230-235	An_{89} - An_{98}
	12070-24	Colorless transparent angular fragments, 520-200μm; light to dark grey opaque grains, 580-200μm	7	228-232	An_{85} - An_{92}
	10085-46	Chalky-white grain 2800 x 1400μm; dark grey granular grain, 1500μm; colorless transparent angular fragments, 250-175μm	6	226-237	An_{81} - An_{100}

Table 3. Analyses of mineral separates from lunar rocks and dusts (con.).

Mineral Isolated	Sample Source*	Description of mineral separates**	Number of analyses	Analytical frequencies cm^{-1}	Derived composition
Olivine	12018-26	Yellow transparent equant grains, 400-170μm; white granular opaque grains, composited with pyroxene, 350μm	3	398	Fa_{33}
	12020-26	Yellow transparent equant grains, 570μm	1	400	Fa_{29}
	12070-24	Light yellow transparent angular fragments, 470-270μm; brown translucent grain, 1000 x 1000μm; brown opaque blocky grain, 1000 x 1000μm	4	401-397	Fa_{28} - Fa_{34}
	10085-46	Grey fine-grained blocky particle, composited with pyroxene, 1500 x 1000μm	1	400	Fa_{29}

Table 3. Analyses of mineral separates from lunar rocks and dusts (con.).

Mineral Isolated	Sample Source*	Description of mineral separates**	Number of analyses	Analytical frequencies cm^{-1}	Derived composition
Ilmenite	12018-26	Black lustrous grains, 100μm	1		
	12021-24	Black lustrous grains, 100μm	1		
	10085-46	Black lustrous grains in aggregates with colorless transparent plagioclase and amber transparent pyroxene, 100μm	1		

*Lunar samples were classified as follows: rock 12018-26, olivine dolerite; rock 12020-26, olivine basalt; rock 12021-24, pigeonite dolerite to porphyritic gabbro with variolitic texture; dust 12001-60, selected sample; dust 12057-57, documented sample; dust 12070-24, contingency sample; dust 10085-46, fines to coarse fines.

**sizes are given as weighted average particle sizes for the analyses.

Table 4. Infrared absorption data for composite samples from lunar dusts

Sample description	Frequency, cm^{-1} Si-O stretching region	Frequency, cm^{-1} Si-O-Si bending region
Dust 12001-60:		
+200 -100 Mesh sieved fraction	985	487
+325 -200 Mesh sieved fraction	990	485
+400 -325 Mesh sieved fraction	1,000	485
-400 Mesh residue	980	470
Dust 12057-57:		
+200 -100 Mesh sieved fraction	980	480
+325 -200 Mesh sieved fraction	980	480
+400 -325 Mesh sieved fraction	990	485
-400 Mesh residue	1,000	485
Dust 12070-24:		
+200 -100 Mesh sieved fraction	985	472
+325 -200 Mesh sieved fraction	985	475
+400 -325 Mesh sieved fraction	987	473
-400 Mesh residue	990	467
8 individual basaltic grains from +100 mesh sieved fraction	1005-990	495-480

Table 4. Infrared absorption data for composite samples from lunar dusts

Sample description	Frequency, cm^{-1}	
	Si-O stretching region	Si-O-Si bending region
Dust 10085-46:		
20 individual basaltic grains from +100 mesh sieved fraction	1005-975	500-475
-100 mesh sieved fraction	990	492
Lunar glass:		
Dust 10085-46, light green	1,000	467
Dust 10085-46, reddish-brown	972	485
Dust 10085-46, dark-brown	970	478
Dust 10085-46, dark-brown	965	480
Dust 10085-46, dark-brown, vesicular	960	480
Dust 12070-24, light green	990	468
Dust 12070-24, reddish-brown beads	970	480

FIGURE CAPTIONS

Fig. 1 Infrared spectra of the predominant silicate minerals in lunar samples. (a) plagioclase (An_{100}) from dust 10085-46, single chalky-white grain, 2800 x 1400μm. (b) pyroxene (Fs_{24}) phenocrysts from rock 12021-24, 15 yellow transparent angular fragments, avg. 600μm. (c) olivine (Fa_{32}) from rock 12018-26, 134 yellow transparent equant grains, avg. 170μm.

Fig. 2 Spectral comparison of lunar pyroxene with synthetic pigeonites. (a) synthetic $Wo_{10}En_{75}Fs_{15}$ (b) synthetic $Wo_{10}En_{60}Fs_{30}$ (c) lunar pyroxene (Fs_{32}) from rock 12018-26, 104 dark amber fragments (d) synthetic $Wo_{10}En_{52}Fs_{38}$ (e) synthetic $Wo_{10}En_{30}Fs_{60}$.

Fig. 3 Determinative curve for synthetic pyroxenes, for he absorption band shifting 400 to 368 cm^{-1} for $Wo_{10}En_{75}Fs_{15}$ to $Wo_{10}En_{30}Fs_{60}$.

Fig. 4 Variation of the Si-O stretching frequency with SiO_2 content for igneous silicate rocks and glasses.

Fig. 4 (con.)

A = 42 chondritic meteorites, using $\%SiO_2$ range from UREY (1953)

B = (a) 15 basalts, mostly tholeiitic: ocean basalt from the East Pacific Rise (Amph 3M, S. R. Hart, Carnegie Institution of Washington); Puerto Rico Trench basalt (No. 5, S. R. Hart); and other Atlantic and Pacific ocean basalts (W. W. Schneider and P. B. Helms, Scripps Institution of Oceanography).

(b) 8 synthetic pseudo-lunar glasses (54-46 $\%SiO_2$, C. H. Greene, Alfred University).

(c) Serpentine (TC-5, D. E. Fogelson, USBM, Minneapolis, Minnesota).

(d) 2 eucrites: Sioux County, Nebraska and Pasamonte, New Mexico (C. B. Moore, Arizona State University), using $\%SiO_2$ range from UREY (1953).

(e) Laminated gabbro from the Romanche Trench (NMNH 110753, V. T. Bowen, Smithsonian Institution) and Fe-Ti rich gabbro (No. 27, Adirondacks, R. B. Hargraves, Princeton University)

C = 23 basalts, mostly alkali-rich; 7 from the Afar Triangle, Ethiopia (F. Barberi, University of Pisa, Italy); Greenland Disco basalt (No. 53479, W. G. Melson, Smithsonian Institution); Puerto Rico Trench basalts (No. 14, S. R. Hart), (F. B. Wooding, Woods Hole Oceanographic Institution); and other Atlantic and Pacific ocean basalts (AD4-1, S. R. Hart), (W. W. Schneider), (P. B. Helms).

D = 9 acid rocks and glasses; including 7 simulated lunar rocks of rhyolites, dacite, granodiorite, pumic, tuff, and obsidian (D. E. Fogelson).

E = 24 tektites; including Javanites, Australites, Indochinites, Moldavites, and Philippinites, using $\%SiO_2$ range from MASON (1962).

F = 7 high-silica glasses, commercial products.

Fig. 5 Infrared spectra of (a) lunar basalt from dust 12070-24, 2 light-grey microgranular aggregates, 1000 and 600μm (b) ocean tholeiitic basalt from the Pacific Antarctic Ridge (No. 21-7-102B, T. E. Simkin, Smithsonian Institution) (c) chondritic meteorite, Plainview, Texas, (d) Javanite, Sangiran Dome Central Java.

Fig. 6 Infrared spectra of samples from lunar dust 12070-24. (a) pyroxene (Fs_{27}), 28 transparent medium-amber angular fragments, avg. 300μm (b) microgranular aggregates, 11 light-grey aggregates, 1700 to 400μm (c) dust sieved fraction +325 -200 mesh.

Fig. 7 Spectral comparison of lunar glass with a tektite and a pseudo-lunar glass. (a) Indochinite, Khon Kaen, Thailand (b) pseudo-lunar glass No. M-17 (C. H. Greene, 45% SiO_2, 15% CaO, 14% Al_2O_3, 10.3% FeO, 0.8% Fe_2O_3, 8% TiO_2, 4% MgO, and 0.08% Na_2O) (c) lunar glass from dust 10085-46, single dark-brown vesicular fragment, 1500 x 1000μm.

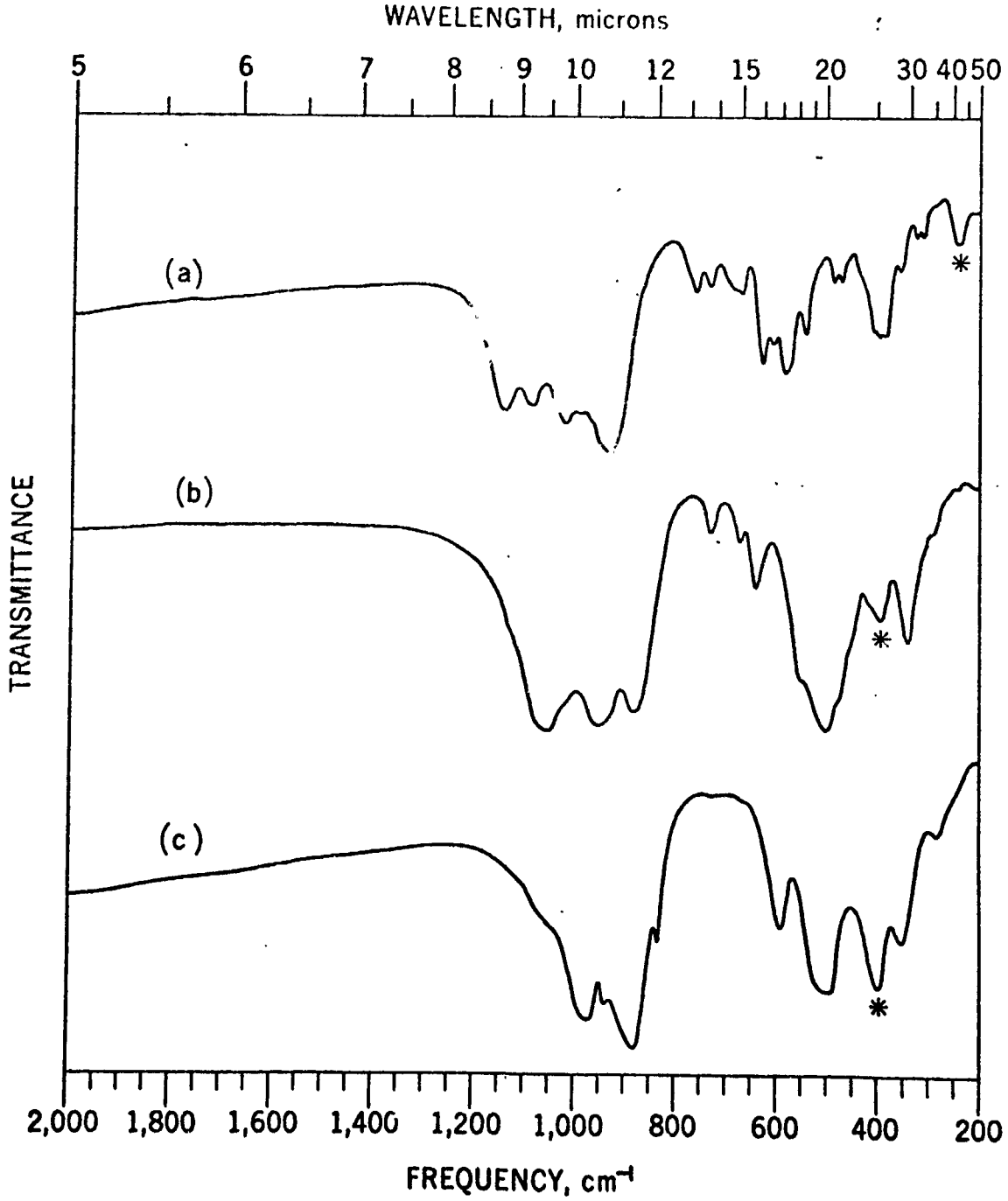
WAVELENGTH, microns
5
6
7
8
9
10
12
15
20
30
40
50
(a)
(b)
(c)
TRANSMITTANCE
2,000
1,800
1,600
1,400
1,200
1,000
800
600
400
200
FREQUENCY, cm⁻¹

Fig. 1

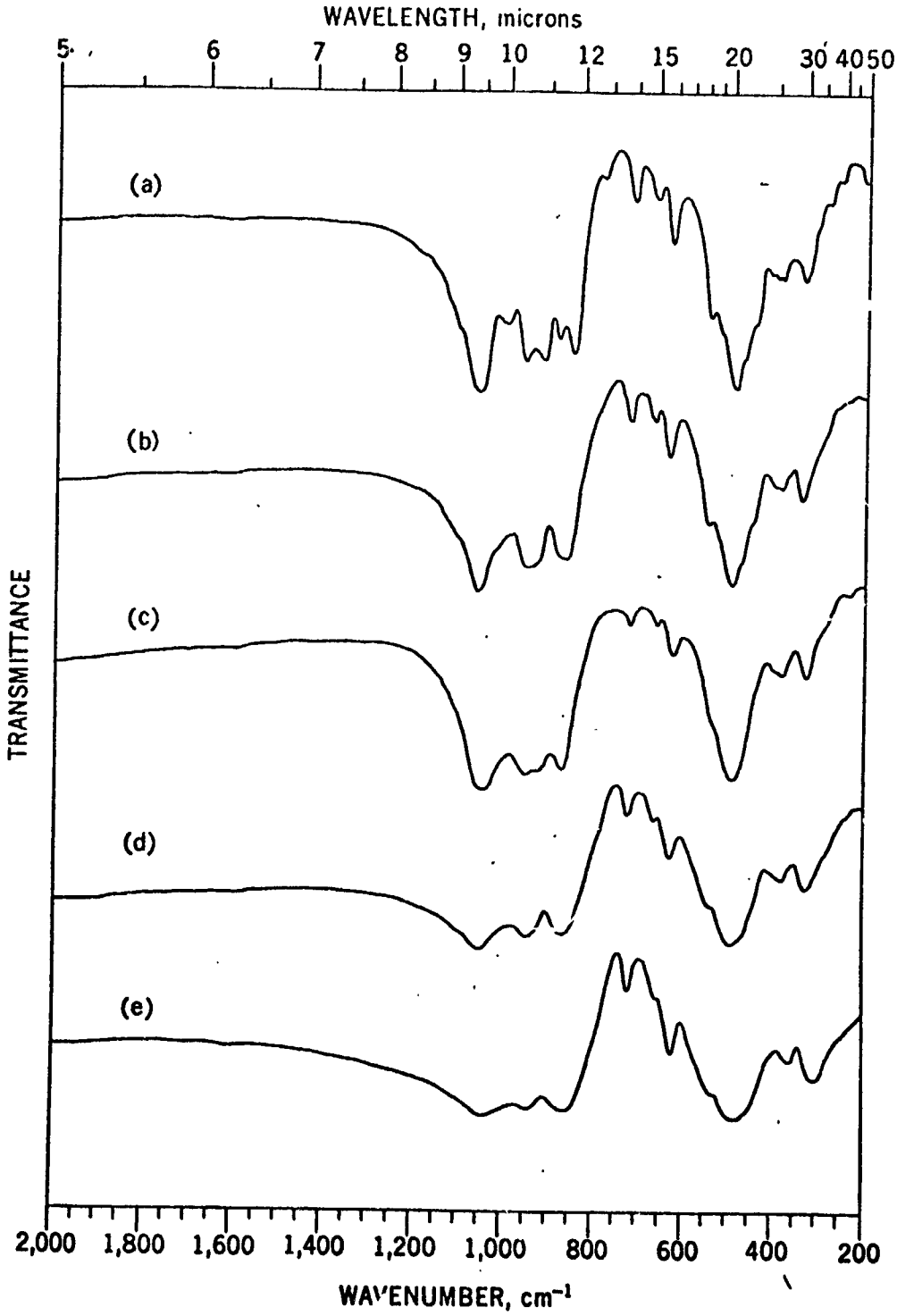
WAVELENGTH, microns
5
6
7
8
9
10
12
15
20
30
40
50
(a)
(b)
(c)
(d)
(e)
TRANSMITTANCE
2,000
1,800
1,600
1,400
1,200
1,000
800
600
400
200
WAVENUMBER, cm⁻¹

Fig. 2

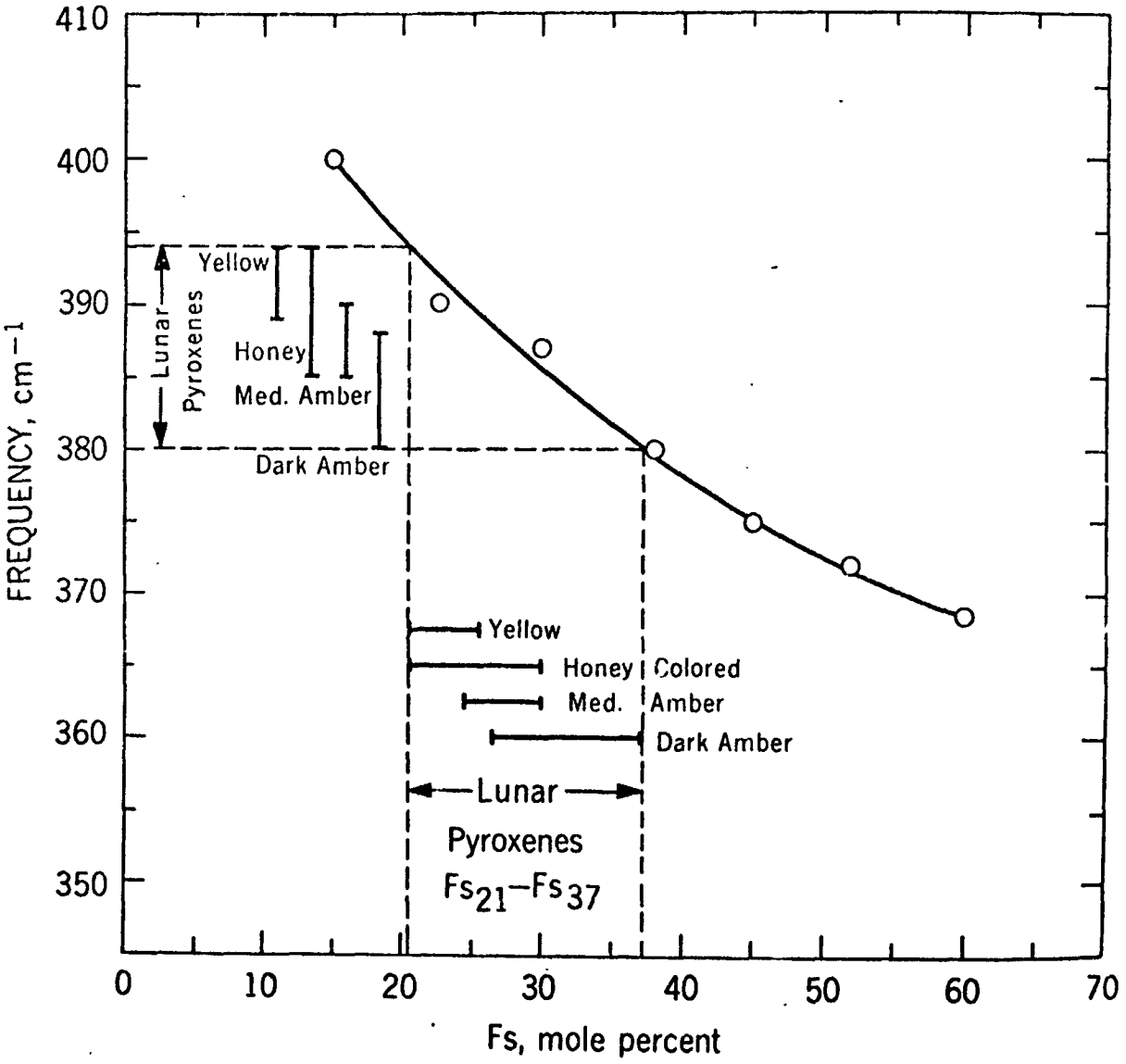
410
400
390
380
370
360
350
FREQUENCY, cm⁻¹
Lunar Pyroxenes
Yellow
Honey
Med. Amber
Dark Amber
Yellow
Honey
Med.
Dark Amber
Colored
Amber
Lunar
Pyroxenes
Fs21–Fs37
0
10
20
30
40
50
60
70
Fs, mole percent

Fig. 3

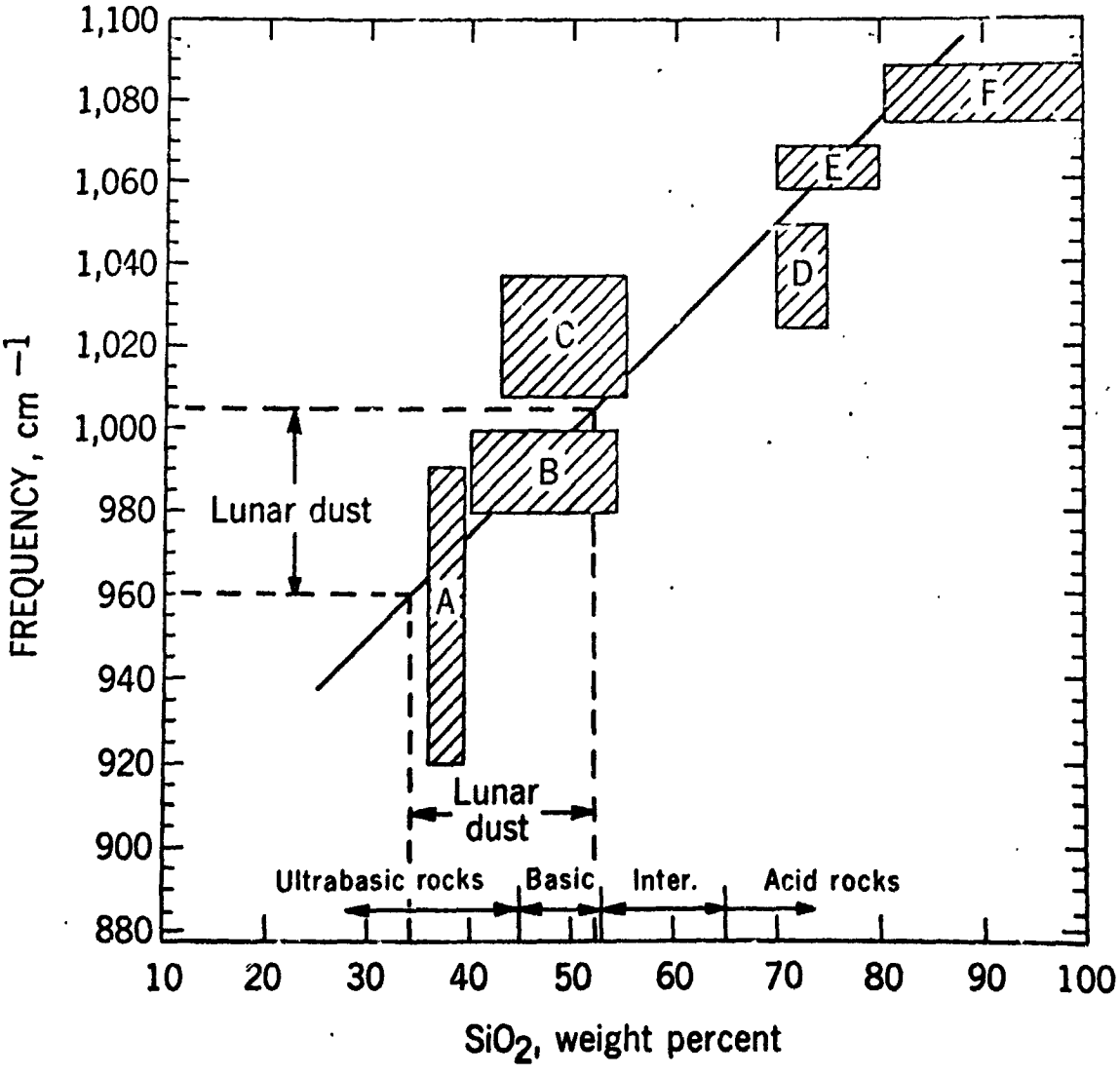
1,100
1,080
1,060
1,040
1,020
1,000
980
960
940
920
900
880
FREQUENCY, cm −1
A
B
C
D
E
F
Lunar dust
Lunar dust
Ultrabasic rocks
Basic
Inter.
Acid rocks
10
20
30
40
50
60
70
80
90
100
SiO2, weight percent

Fig. 4

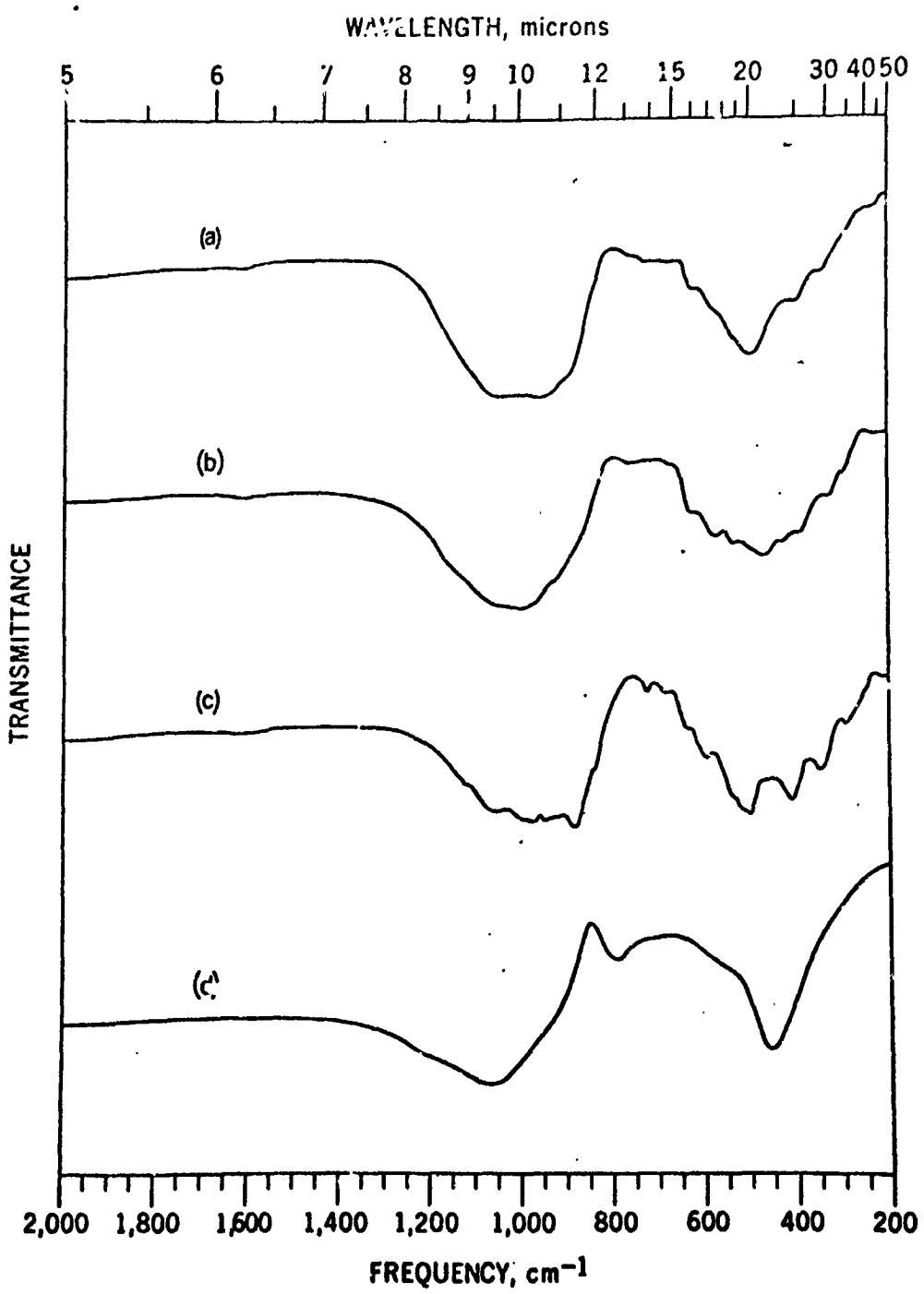
WAVELENGTH, microns
5
6
7
8
9
10
12
15
20
30
40
50
(a)
(b)
(c)
(d)
TRANSMITTANCE
2,000
1,800
1,600
1,400
1,200
1,000
800
600
400
200
FREQUENCY, cm⁻¹

Fig. 5

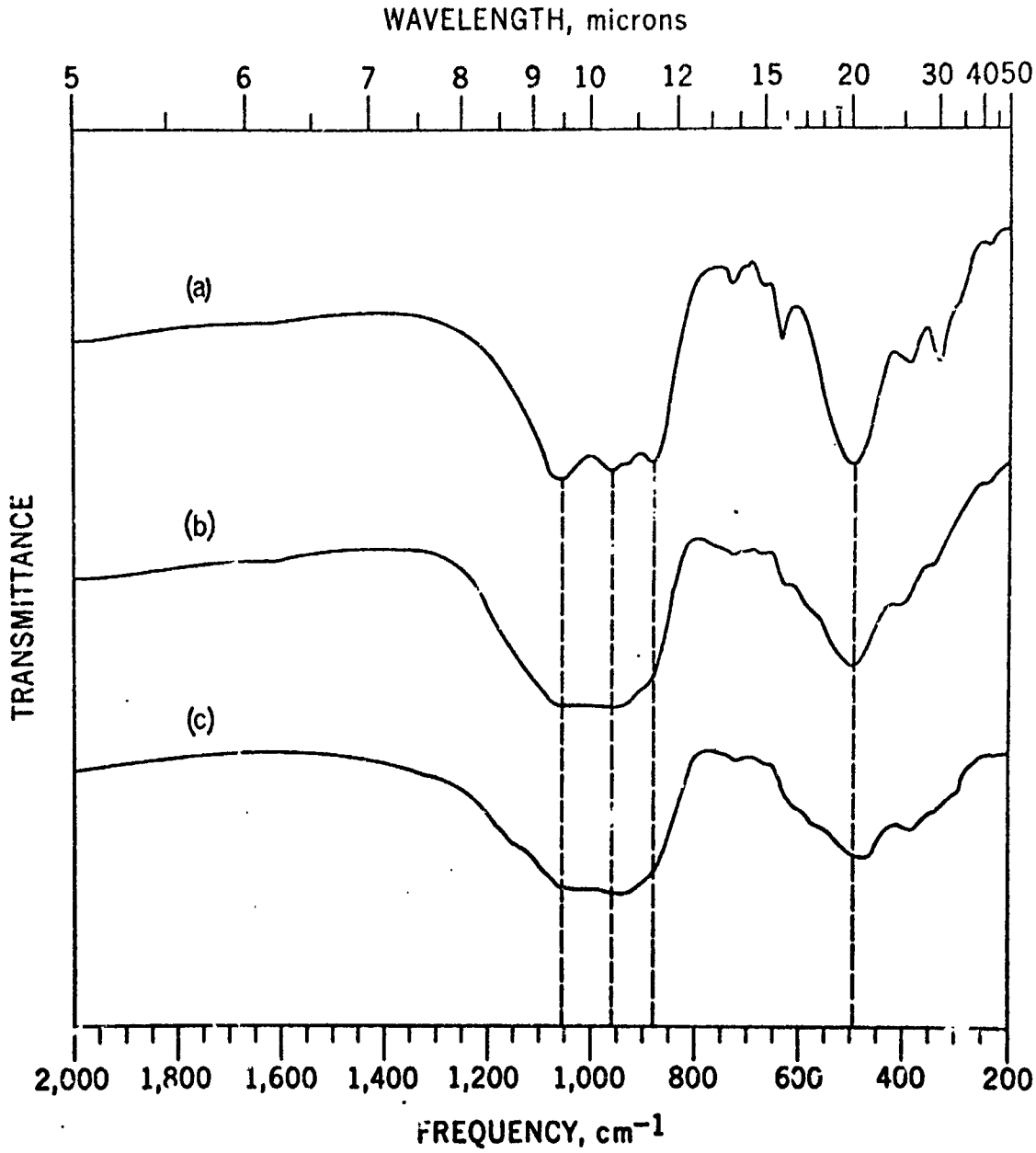
WAVELENGTH, microns
5
6
7
8
9
10
12
15
20
30
40
50
(a)
(b)
(c)
TRANSMITTANCE
2,000
1,800
1,600
1,400
1,200
1,000
800
600
400
200
FREQUENCY, cm⁻¹

Fig. 6

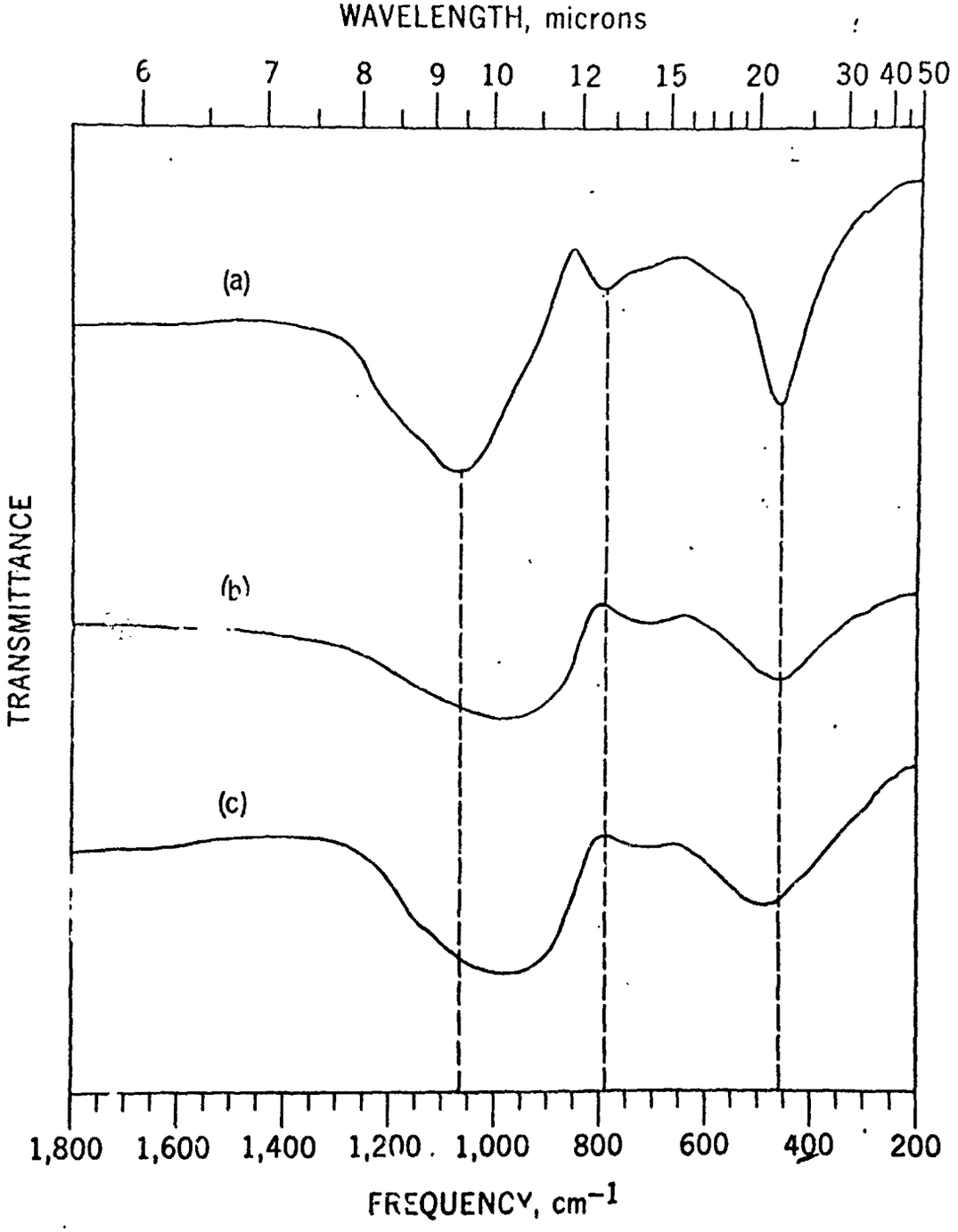
WAVELENGTH, microns
6
7
8
9
10
12
15
20
30
40
50
(a)
(b)
(c)
TRANSMITTANCE
1,800
1,600
1,400
1,200
1,000
800
600
400
200
FREQUENCY, cm⁻¹

Fig. 7